Crystal Morphology and Nonisothermal Crystallization Kinetics of Short Carbon Fiber/Poly(trimethylene terephthalate) Composites

Mingtao Run, Hongzan Song, Chenguang Yao, Yingjin Wang

College of Chemistry and Environmental Science, Hebei University, Baoding 071002, China

Received 1 March 2007; accepted 1 May 2007
DOI 10.1002/app.26661
Published online 29 June 2007 in Wiley InterScience (www.interscience.wiley.com).

ABSTRACT: The crystal morphology and nonisothermal crystallization kinetics of short carbon fiber/poly(trimethylene terephthalate) (SCF/PTT) composites were investigated by polarized optical microscopy (POM) and differential scanning calorimetry (DSC). The optical micrographs suggest that the more content of SCF in composites, the smaller size of the spherulites is. Moreover, the addition of SCF can lead to forming banded spherulites in composites. The Avrami equation modified by Jeziorny, Ozawa theory and the method developed by Mo were used, respectively, to fit the primary stage of nonisothermal crystallization of various composites. The results suggest that the SCF served as nucleation agent, accelerates the crystallization rate of the composites, and the more content of SCF, the faster crystallization rate is. Effective activation energy calculated by the differential iso-conversional method developed by Friedman also concludes that the composite with more SCF component has higher crystallization ability than that with less SCF content. The kinetic parameters U^* and K_g are determined, respectively, by the Hoffman–Lauritzen theory. © 2007 Wiley Periodicals, Inc. J Appl Polym Sci 106: 868–877, 2007

Key words: poly(trimethylene terephthalate); short carbon fiber; banded spherulites; nonisothermal crystallization kinetics; DSC

INTRODUCTION

Poly(trimethylene terephthalate) (PTT) has become a commercial engineering thermoplastic material with the breakthrough in 1,3-propanediol manufacturing cost.[1] Compared with the other familiar polyesters, such as poly(ethylene terephthalate) (PET) and poly (butylene terephthalate) (PBT), PTT has strong competitive power due to its excellent properties on mechanics and electrics.[2] Since its commercialization in 1998, PTT has received much attention from the famous corporation internal or external and research institution.[3–7]

Since both physical and mechanical properties of a semi-crystalline polymer are strongly dependent on the extent of crystallization and morphology developed during processing, studies related to crystallization kinetics are key information to gain an understanding on the interrelationship of processing-structure-property.[8] Studies related to the chain conformation, crystal structure, and morphology of PTT have been carried out and reported in recent years.[9] There are many publications concerning isothermal and nonisothermal crystallization kinetics of pure PTT and its blend with PBT, PET, and clay nanocomposites, etc.[10–15] The effect of fibers on crystallization of semi-crystalline thermoplastics is a major concern in polymer science because of the technical importance of fiber-reinforced composites.[16] The important studies on carbon fiber reinforced polymer composites include CF/PEEK,[17,18] CF/PP,[19] CF/PEI,[20,21] et al. However, to our knowledge no experimental about effects of the SCF on the nonisothermal crystallization behaviors of PTT have been reported.

In the present study, composites of SCF/PTT were prepared and characterized for their crystal morphology and nonisothermal crystallization kinetics by using POM and DSC measurements. The experiment data were analyzed based on the Avrami equation modified by Jeziorny, Ozawa theory and the method developed by Mo. The effective activation energy was calculated by the differential iso-conversional method developed by Friedman. Moreover, U^* and K_g were also determined by the Hoffman–Lauritzen theory.

EXPERIMENTAL

Materials

PTT homopolymer was supplied in pellet form by Shell Chemicals (USA) with an intrinsic viscosity of 0.90 dL/g measured in a phenol/tetrachloroethane solution (50/50, w/w) at 25°C. Short carbon fiber with epoxy sizing

Correspondence to: M. Run (rmthyp@hotmail.com).
Contract grant sponsor: Natural Science Foundation of Hebei Province; contract grant number: B2007000148.
Contract grant sponsor: Hebei University; contract grant number: Y2006065.

Journal of Applied Polymer Science, Vol. 106, 868–877 (2007)
©2007 Wiley Periodicals, Inc.

(B-DJ04S) used in our experiment was a PAN-based type supplied by Anbaoli Co. (China) with a diameter of 7 μm and an average length of 4 mm.

Composites preparation

PTT were dried in a vacuum oven at 100°C for 12 h and the SCF were dried in oven at 70°C for 24 h before preparing composites. PTT and SCF were mixed together with different weight ratio of SCF/PTT as follows: A0: 0/100; A1: 1/99; A2: 2/98; A3: 5/95; A4: 10/90, and then melt-blended in a ZSK-25WLE WP self-wiping, co-rotating twin-screw extruder, operating at a screw speed of 100 rpm and at a die temperature of 260°C. The resultant composite ribbons were cooled in cold water, cut up, re-dried before being used in measurements.

Polarized optical microscopy (POM)

POM (Yongheng 59XA, China) with a digital camera system (Panasonic wv-CP240, Japan) was used for observation of the crystal morphology. Samples were pressed between two glass slides with a distance of about 200 μm and first melted on a hot stage at 260°C for 10 min, and then cooled to room temperature at a cooling rate of 1°C/min. Taking photographs at different time for each sample. It should be noted that the crystallization time for PTT (A0) is 64 min, whereas 45, 35, 28, and 18 min for A1, A2, A3, and A4, respectively; however, the morphology of all crystalline samples is nearly unchangeable with the time going longer than these times.

Differential scanning calorimetry (DSC)

The nonisothermal crystallization behaviors were performed on the Perkin–Elmer Diamond DSC instrument that calibrated with indium prior to performing the measurement, and the weights of all samples were approximately 6.0 mg. The sample was heated to 260°C in nitrogen, held for 5 min and then cooled to 30°C at constant cooling rates of 5, 10, 15, 20, 30, 40°C/min, respectively. The exothermic curves of heat flow as a function of temperature were recorded and investigated.

RESULTS AND DISCUSSION

Crystal morphology analysis

When samples are cooled from molten state at a cooling rate of 1°C/min, nucleus are observed at specific nucleation temperature in different sample, i.e., the nucleus of A0, A1, A2, A3, and A4 appear at 205, 209, 210, 212, and 214°C, respectively, indicating that the SCF is a good nucleation agent for the crystallization of PTT. For each sample, the time when the crystal nucleus is observed is set as $t = 0$. The crystal photographs of each composite crystallized at different time are shown in Figure 1.

In Figure 1(a,b), many perfect Maltese crosses are observed in A0. The largest one with a diameter of 80 μm is formed within 29 min [in Fig. 1(a)], and their final dimension reaches large beyond 150 μm with 64 min [in Fig. 1(b)]. Without the nucleation agent of SCF, the crystallization process of A0 is slowly by homogenous nucleation mode and three-dimensional crystal growth. The spherulites' size can reach very large, since the number of nucleus is small in the limited space between the two glass slides.

As shown in Figure 1(c,d), the micrographs of A1 sample with SCF of 1 wt %, some of spherulites formed with SCF through heterogeneous nucleation mode and grow fast with a larger dimension of about 80 μm within 18 min [as shown by the arrow in Fig. 1(c)]; whereas others still grow through thermal or athermal nucleation mode with the slow growth rate of smaller dimension. In Figure 1(d), the dimension of spherulite is about 130 μm (as shown by the arrow) within 45 min. But the final average size of spherulite in this sample is smaller than that of A0, which due to more nucleus formed in the limited space and different spherulites will impinge each other in growing process. Moreover, the crystals of A1 are mostly banded spherulites, especially those formed with SCF.

With the increasing content of SCF in composites, as shown in Figure 1(e,g,m), it can be seen that nearly most spherulites are firstly formed around SCF and their nucleation mode should predominantly be heterogeneous nucleation. As shown in Figure 1(f,h,n), the concentric banded rings are also observed in the final spherulites. It should be noted that the average dimension of the spherulites is decreased with increasing content of SCF in composites, e.g., the average spherulite dimension of A1, A2, A3, and A4 is about 130, 110, 100 and 70 μm, respectively. Therefore, it can be concluded that SCF acting as nucleation agent can not only accelerates the crystallization rate but also decreases the dimension of the crystals; moreover, it can bring banded spherulites due to the interaction between the SCF and PTT molecular chains at this cooling condition.

Nonisothermal crystallization kinetics analysis

Analysis based on the Avrami theory modified by Jeziorny

The relative crystallinity (X_t) as a function of temperature is defined as the following equation:

$$X_t = \frac{\int_{t_0}^{t} (dH/dt)dt}{\int_{t_0}^{t_\infty} (dH/dt)dt} \quad (1)$$

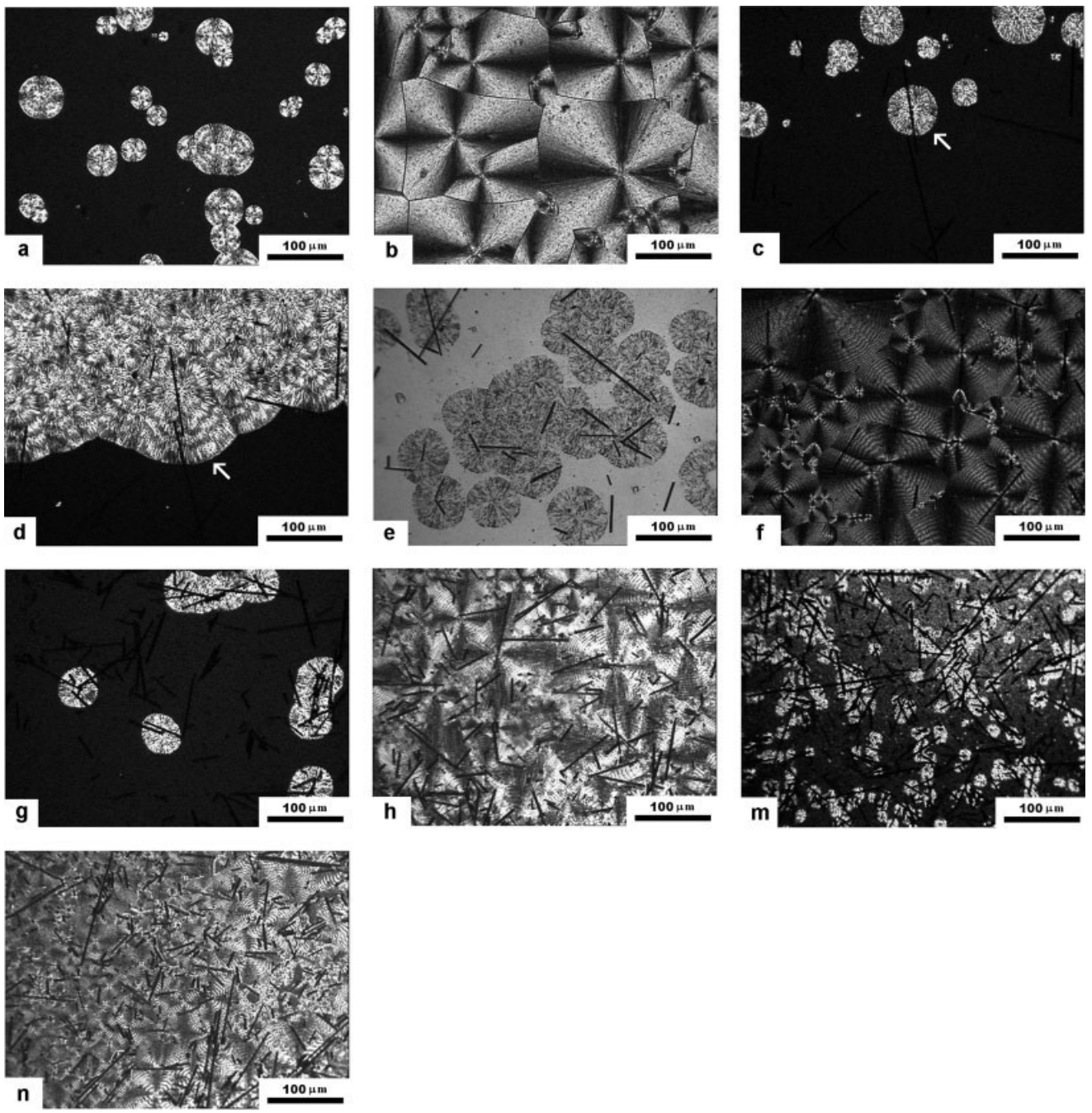

Figure 1 POM micrographs of the composites crystallized at different time. A0: (a) 29 min, (b) 64 min, A1: (c) 18 min, (d) 45 min, A2: (e) 14 min, (f) 35 min, A3: (g) 11 min, (h) 28 min, A4 (m) 6 min, (n) 18 min.

where the dH/dT is the rate of heat evolution, t_0 and t_∞ are the time, at which crystallization starts and ends, respectively.

The relationship between temperature T and time t is given by (2) during the nonisothermal crystallization process, as follows:

$$t = \frac{|T_0 - T|}{D} \tag{2}$$

where t is the crystallization time, T_0 is the temperature at which crystallization begins ($t = 0$), T is the temperature at a crystallization time t, and D is the cooling rate.

In this study, the samples of A0, A1, and A4 are selected to study their nonisothermal crystallization kinetics. The nonisothermal crystallization exothermic peaks of A0 and A4 composites at various cooling rate are shown in Figure 2, and their parameters are summarized in Table I. The exothermic peak

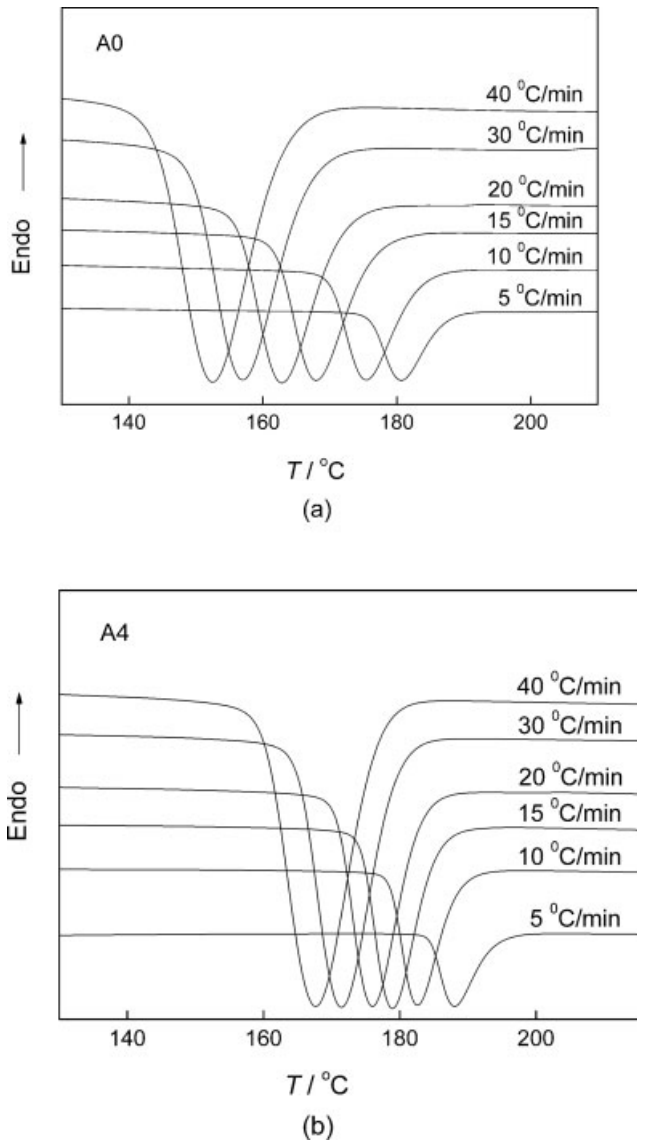

Figure 2 Nonisothermal crystallization curves of (a) A0 and (b) A4 composites at different cooling rates.

temperature, T_{cp}, shifts to lower temperature region with increasing cooling rates from 5 to 40°C/min, e.g., T_{cp} of A0, A1, and A4 shifts to lower temperature about 29.0, 28.1, and 22.3°C, respectively. This result indicates that the more content of SCF in composite, the less influence of the cooling rate on crystallization. From the DSC digital information, X_t is calculated at different temperature, and the plots of X_t versus T are shown in Figure 3(a,b).

According to (2) the horizontal T-axis in Figure 3 can be transformed into the crystallization time t-axis as shown in Figure 4(a,b). It can be seen from Figure 4 that all these curves have similar sigmoidal shape, and the curvature of the upper parts of the plot is observed to be level off due to the spherulites impingement that already begin from the inflection point of the curves. The characteristic sigmoidal

TABLE I
Nonisothermal Crystallization Kinetic Parameters of A0, A1, and A4 Analyzed by Modified Avrami Equation

	A0					A1					A4				
D (°C/min)	T_{cp} (°C)	n	$t_{1/2}$ (min)	K_c (10^{-4} s^{-n})	ΔH_c (J/g)	T_{cp} (°C)	n	$t_{1/2}$ (min)	K_c (10^{-4} s^{-n})	ΔH_c (J/g)	T_{cp} (°C)	n	$t_{1/2}$ (min)	K_c (10^{-4} s^{-n})	ΔH_c (J/g)
5	180.5	3.1	4.4	295	−51.1	189.7	5.0	2.3	94	−50.1	190.0	5.5	2.2	596	−48.1
10	172.6	3.1	2.6	2010	−50.0	178.7	4.9	1.5	116	−49.1	182.6	5.4	1.3	946	−46.6
15	166.1	2.9	1.8	4070	−47.2	175.9	4.8	1.1	168	−48.2	179.0	5.3	0.92	1144	−46.4
20	160.4	2.8	1.5	5090	−43.6	171.8	4.7	0.83	241	−46.0	176.0	4.7	0.67	1687	−45.6
30	156.3	2.8	1.2	6380	−34.8	166.1	4.6	0.61	327	−45.6	171.4	4.7	0.53	1890	−45.4
40	151.5	2.7	0.88	7310	−21.9	161.6	4.4	0.49	473	−44.4	167.7	4.5	0.37	2922	−43.6

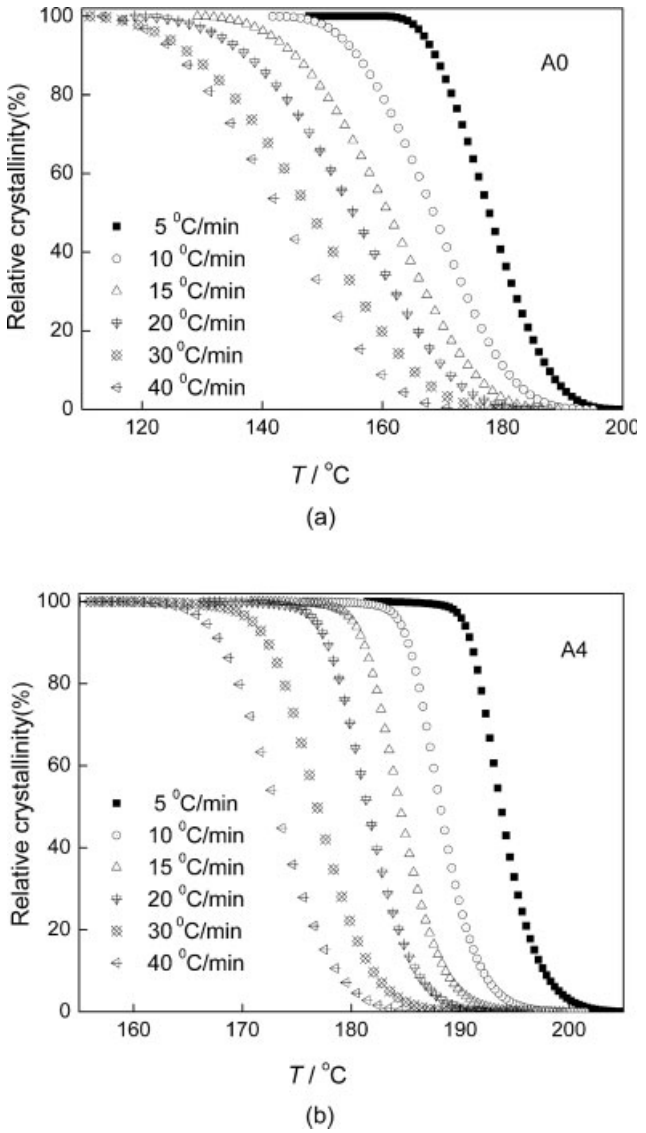

Figure 3 Relative crystallinity vs. temperature for nonisothermal crystallization of (a) A0 and (b) A4 composites.

curves are shifted to lower temperature or shorter time with increasing cooling rates for completing the crystallization. Through Figure 4(a,b), we can get the half time of crystallization, $t_{1/2}$, when the X_t are equal to 50%, and the parameters are listed in Table I. It can be seen that $t_{1/2}$ values decrease with increasing cooling rates, indicating a faster crystallization rate with increasing cooling rate. Moreover, compared the values of $t_{1/2}$ of A0 with those of A1 and A4 at a given cooling rate, it is clear that the SCF accelerates the crystallization rate of PTT, and the more SCF component in composites, the higher crystallization rate is.

The primary stage of nonisothermal crystallization could be described by Avrami equation,[22,23] based on the assumption that the crystallization temperature is constant; it can be obtained the following:

$$1 - X_t = \exp(-K_t t^n) \tag{3}$$

$$\log [-\ln (1 - X_t)] = n \log t + \log K_t \tag{4}$$

where K_t is a growth rate constant involving both nucleation and growth rate parameters. Jeziorny[23] considered the values of K_t determined by Avrami equation should be adequate as follows:

$$\log K_c = \frac{\log K_t}{|D|} \tag{5}$$

where K_c is the kinetic crystallization rate constant.

Figure 5(a,b) shows a series of double logarithm plots of $\log [-\ln (1 - X_t)]$ vs. $\log t$ at different cooling rates. Each curve in Figure 5 shows good linearity

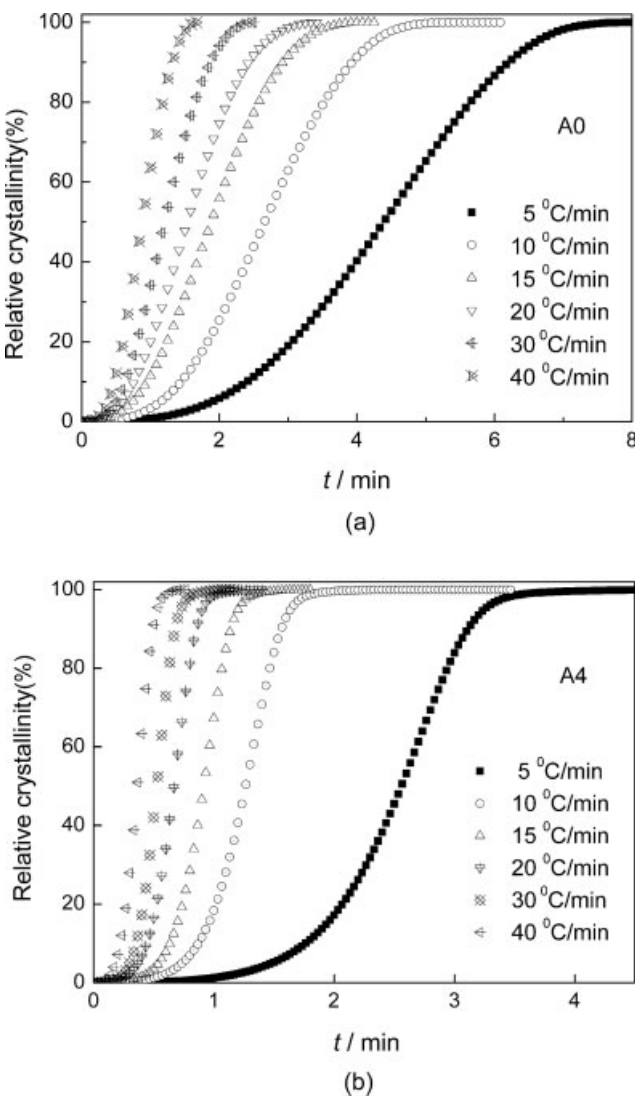

Figure 4 Relative crystallinity vs. time for nonisothermal crystallization of (a) A0 and (b) A4 composites.

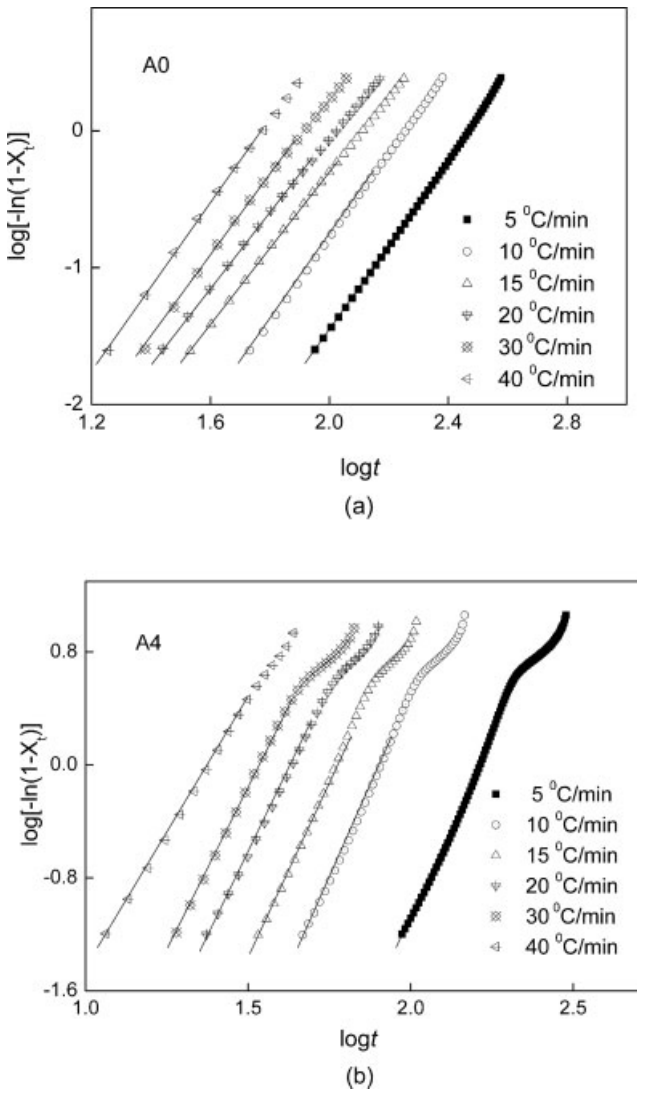

Figure 5 Plots of $\log[-\ln(1-X_t)]$ vs. $\log t$ for nonisothermal crystallization of (a) A0 and (b) A4 composites.

except a secondary crystallization at the later crystallization stage. The Avrami exponent n and K_c of A0, A1 and A4 obtained from the slopes and the intercepts are listed in Table I, respectively.

The Avrami exponent, n, are found to range from 3.1 to 2.7 for PTT, from 5.0 to 4.4 for A1 and from 5.5 to 4.5 for A4 when cooling rates increase from 5 to 40°C/min. The values of n decrease gradually with increasing cooling rate for each sample, indicating that the crystallization growth is on fewer dimensions with increasing cooling rate. Judged from the n of neat PTT, its nucleation type should predominantly by homogenous thermal nucleation and its crystal growth should dominantly change from three-dimensional to two-dimensional crystal growth with increasing cooling rate. However, for A1 and A4 with heterogeneous nucleus, the values of exponent n are between 4.4 and 5.5 at various cooling rates, which is not consist with the supposing of the Avrami theory. This result may due to the spherulites' impingement and crowding, or the complicated nucleation types and growth form of spherulites.[24] And it is known that the nucleation mode is dependent on the cooling rate.[25] Nevertheless, considering the results of the crystal morphology in Figure 1 for the SCF/PTT composites, its nucleation type should mostly be a heterogeneous nucleation and its crystal growth dimension should mostly be three-dimensional space extension.

It can be clearly seen in Table I that K_c increases as a function of D, and SCF/PTT composites have a higher value of K_c than that of pure PTT at a given cooling rate. These results suggest that the crystallization rate is accelerated greatly with the addition of SCF, and the more SCF content in composites, the higher crystallization rate is. Moreover, ΔH_c of each sample is gradually decreased due to the less amorphous polymer turned into crystal form in the composite with increasing cooling rate. At the same cooling rate, ΔH_c of A0, A1, and A4 is decreasing with increasing content of SCF in composites, indicating that the crystallinity is decreased by the SCF.

Analysis based on the Ozawa theory

Since the nonisothermal crystallization is a rate-dependent process, Ozawa[26] took into account the effect of cooling (or heating) rate, D, on the crystallization process from the melt or glassy state, and modified the Avrami equation as follows:

$$1 - X_t = \exp\left[-\frac{K(T)}{|D|^m}\right] \tag{6}$$

$$\log\left[-\ln(1-X_t)\right] = \log K(T) - m\log|D| \tag{7}$$

where $K(T)$ is a function related to the overall crystallization rate that indicates how fast crystallization proceeds, and m is the Ozawa exponent that depends on the dimension of crystals growth. According to the Ozawa's theory and plots of $\log[-\ln(1-X_t)]$ versus $\log|D|$ at a given temperature, a series of straight lines will be obtained if Ozawa analysis is valid, and the crystallization kinetic parameters m and $\log K(T)$ can be derived from the slope and the intercept, respectively.

The results of the Ozawa analysis for A0 and A4 composites are shown in Figure 6(a,b), and a series of straight lines are obtained, and the values of m and $\log K(T)$ are listed in Table II. For each composite, the values of m and $\log K(T)$ are increased with the increasing temperature indicating that the crystallization growth is on more dimensions and at fast

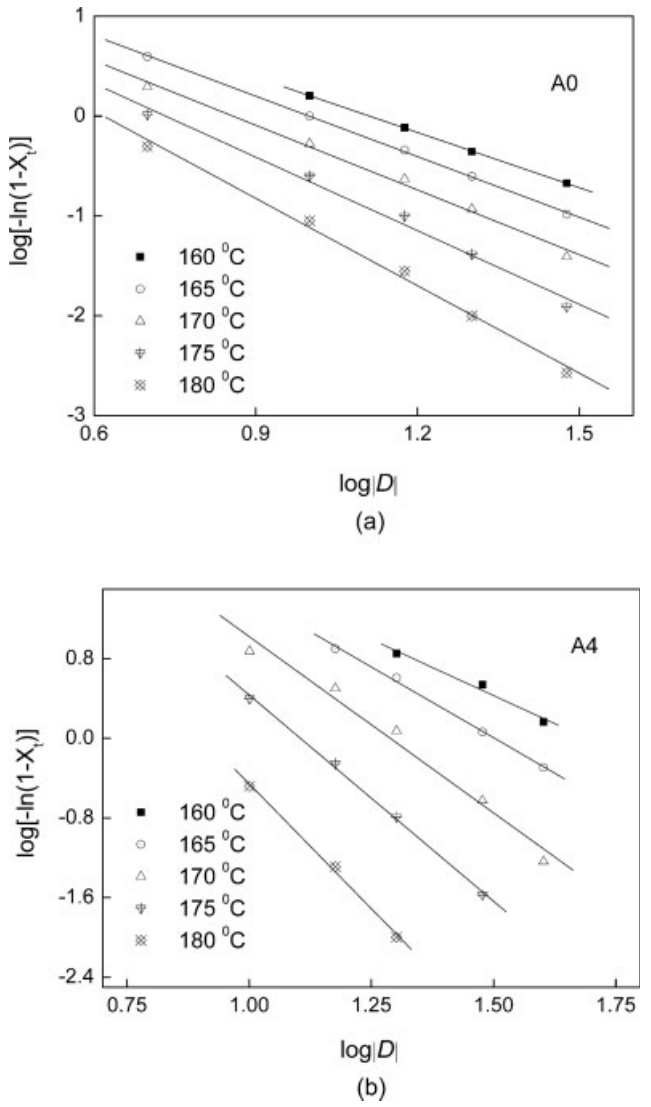

Figure 6 Ozawa plots of $\log[-\ln(1-X_t)]$ vs. $\log|D|$ for (a) A0 and (b) A4 composites.

crystallization rate at the higher temperature, while it is on less dimensions and lower crystallization rate at the lower temperature. Furthermore, compared the values of m and log $K(T)$ of A0 with those of A1 and A4 in the temperature range of 160 to 180°C, it is obvious that the results of A0 is much lower than those of A1 and A4, indicating that SCF can accelerate crystallization rate of PTT, and the more SCF content in composites, the higher the crystal growth dimension and the crystallization rate is.

Analysis based on the Mo theory

Mo et al. proposed a different kinetic equation by combining the Avrami and Ozawa equations.[27] As the degree of crystallinity is related to the cooling rate D and the crystallization time t (or T), the relationship between D and t could be defined for a given degree of crystallinity. Consequently, a new kinetic equation for nonisothermal crystallization was derived by combining Eqs. (4) and (7):

$$\log K_t + n\log t = \log K(T) - m\log|D| \tag{8}$$

$$\log|D| = \log F(T) - b\log t \tag{9}$$

where the parameters $F(T) = [K(T)/K_t]^{1/m}$, and b is the ratio between the Avrami and Ozawa exponents, i.e. $b = n/m$. $F(T)$ refers to the value of cooling rate chosen at unit crystallization time when the system amounted to a certain degree of crystallinity. The smaller the value of $F(T)$, the higher the crystallization rate is. Therefore, $F(T)$ has a definite physical and practical meaning.

According to Mo's method, plots of log $|D|$ against log t at a given degree of crystallinity will give a straight line with an intercept of $\log F(T)$ and a slope of $-b$ if Mo analysis is valid. As shown in Figure 7, plotting log $|D|$ against log t for A0 and A4 composites demonstrate linear relationship at a given X_t, and the values of $\log F(T)$ and $-b$ are listed in Table III. The $\log F(T)$ values are increased with the relative crystallinity from 3.24 to 4.26 (for A0), 3.40 to 3.65 (for A1), and 2.99 to 3.33 (for A4), indicating that a lower crystallization rate is needed to reach the given degree of crystallinity within unit time. The parameters $-b$ shows only a small increase with increasing X_t, ranging from 1.31 to 1.41 (for A0), 1.31 to 1.32 (for A1) and 1.12 to 1.20 (for A4), respectively. Compared the values of log $F(T)$ of A0 with

TABLE II
Nonisothermal Crystallization Kinetic Parameters of A0, A1, and A4 Analyzed by Ozawa Equation

	A0			A1			A4		
T (C)	m	log $K(T)$	r^2	m	log $K(T)$	r^2	m	log $K(T)$	r^2
160	1.8	1.80	0.9969	2.3	3.92	0.9991	2.4	3.99	0.9887
165	2.0	1.81	0.9948	2.8	4.24	0.9959	2.9	4.25	0.9987
170	2.1	1.85	0.9963	3.3	4.46	0.9982	3.5	4.56	0.9892
175	2.5	2.01	0.9997	3.8	4.53	0.9981	4.1	4.58	0.9981
180	2.9	2.05	0.9999	4.5	4.64	0.9996	5.1	4.65	0.9983

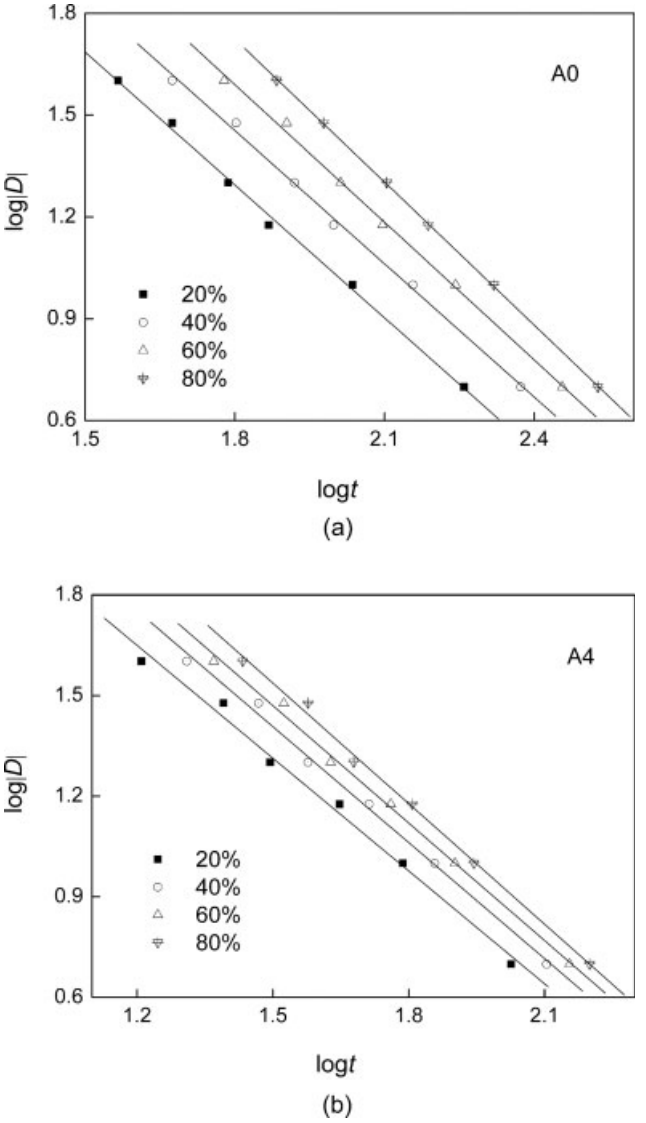

Figure 7 log $|D|$ vs. log t from the Mo equation for (a) A0 and (b) A4 composites.

A1 and A4 at a given X_t, it is obvious that the results of A0 is larger than those of A1 and A4, indicating that SCF accelerates crystallization rate of PTT, and the more SCF content, the higher crystallization rate is. This conclusion is confirmed with those derived from the analysis of Avrami, Ozawa theory and the results of Figure 1. Thus the equation of Mo method successfully describes the nonisothermal crystallization process of SCF/PTT composites.

TABLE III
Nonisothermal Crystallization Kinetic Parameters of A0, A1, and A4 Analyzed by Mo Equation

	A0		A1		A4	
X_t (%)	b	log $F(T)$	b	log $F(T)$	b	log $F(T)$
20	1.32	3.64	1.31	3.40	1.12	2.99
40	1.32	3.81	1.31	3.48	1.15	3.12
60	1.35	4.03	1.31	3.57	1.17	3.22
80	1.41	4.26	1.32	3.65	1.20	3.33

Crystallization activation energy

To obtain the reliable values of the effective activation energy on the melt cooling process, Friedman originated the differential iso-conversional method.[28] The kinetic equation for a given process may be written as $d\alpha/dt = k(T)f(\alpha)$, where $k(T)$ is the Arrhenius constant, α is the conversion degree and $f(\alpha)$ is the function describing the reaction mechanism. When analyzing DSC data, the conversion degree may be defined as $\alpha = H/Q$, where H is the amount of heat involved in a reaction at a conversion degree α, and Q is the total amount of heat involved in the overall reaction. The relation above described, in the logarithm form, is:

$$\ln\left(\frac{d\alpha}{dt}\right)_\alpha = \ln\left(A_\alpha f(\alpha)\right) - \frac{E_\alpha}{RT_\alpha} \tag{10}$$

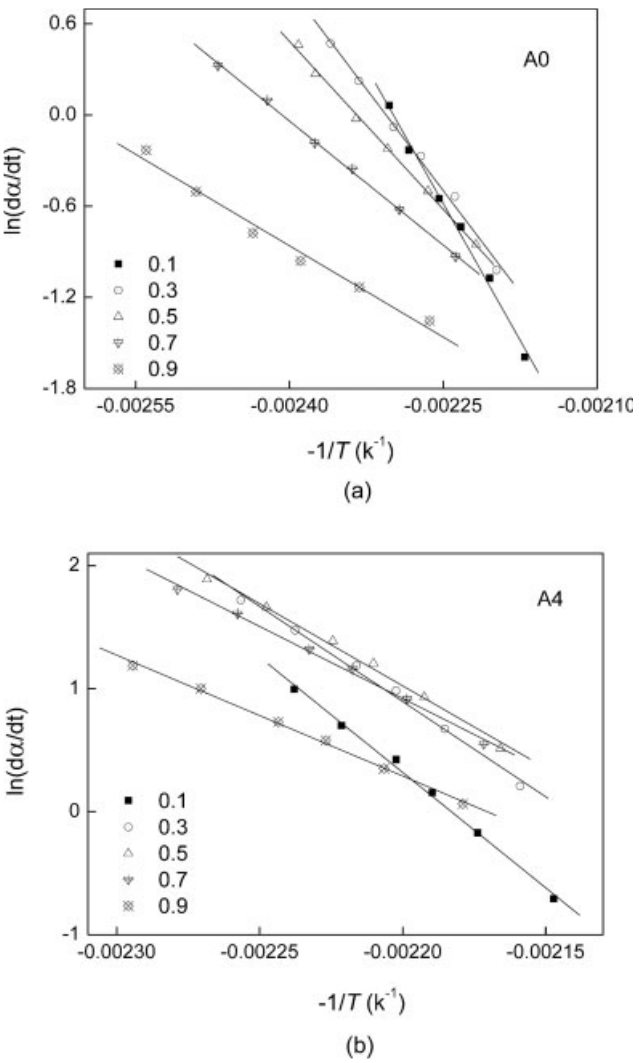

Figure 8 Friedman plots of ln $(d\alpha/dt)$ vs. $1/T$ for (a) A0 and (b) A4 composites.

TABLE IV
Effective Activation Energy of A0, A1, and A4 Composites

	A0	A1	A4
A	E_a (kJ/mol)	E_a (kJ/mol)	E_a (kJ/mol)
0.1	−99.66	−117.98	−155.97
0.3	−84.20	−106.34	−128.72
0.5	−71.35	−99.75	−119.69
0.7	−65.30	−93.28	−114.87
0.9	−53.32	−80.55	−104.22

where A_α, E_α, and T_α are the pre-exponential factor, the effective activation energy and temperature at a certain conversion degree α, respectively.

The analysis by Friedman theory for A0 and A4 composites are shown in Figure 8(a,b). A series of straight lines were obtained, then E_α can be derived from the slope of each line and their values are listed in Table IV. To each composite, the effective activation energy increases from −99.66 to −53.32 kJ/mol for A0, from −117.98 to −80.55 kJ/mol for A1 and from −155.97 to −104.22 kJ/mol for A4 with the extent of α = 0.1–0.9. This result suggests that it is easier for composite to crystallize at the beginning of the crystallization, while it becomes difficult as the crystallization proceed. By comparing the effective activation energy at the same degree conversion, it is easy to find that the effective activation energy of A1 and A4 are more negative than that of A0, which indicates that SCF improves the crystallization ability of the composite. Moreover, the effective activation energy of A4 is more negative than that of A1, suggested that the composite with more SCF component has higher crystallization ability than that with less SCF content.

Because of the different cooling rates, the same value of α is accomplished at different temperatures. We have used the average temperature to associate with α and E_α, thus E_α on α dependence can be converted into the E_α on T dependence that is presented in Figure 9. As shown in Figure 9, the $E_\alpha(T)$ dependence displays a breakpoint at 441 K for A0, 456 K for A1, and 460 K for A4 composite, which may be due to the change in crystallization mechanism. Subject to the change in crystallization mechanism, it makes sense to parameterize the higher temperature and lower temperature portions of the $E_\alpha(T)$ dependence separately. The dependence of $E_\alpha(T)$ of two portions has been performed nonlinear fits of Hoffman–Lauritzen[29] theory and (11) derived by Vyazovkin[30,31] using graphics software Origin 7.0.

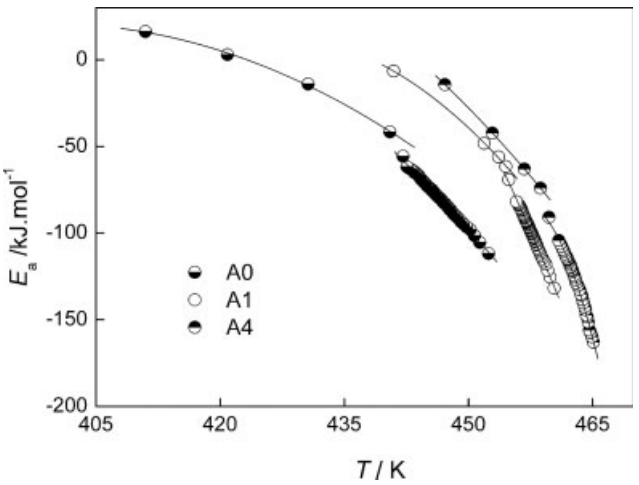

Figure 9 Dependence of the effective activation energy on average temperature. The solid lines represents fits of (11).

$$E_a(T) = U^* \frac{T^2}{(T - T_\infty)^2} + K_g R \frac{T_m^2 - T^2 - T_m T}{(T_m - T)^2 T} \qquad (11)$$

The values of K_g and U^* yielded has been shown in Table V, all fits have been accomplished with the coefficient of determination (r^2) larger than 0.98. From the Table 7, the values of K_g for higher and lower temperature are 1.0×10^5 K^2 and 0.51×10^5 K^2 for A0, 1.04×10^5 K^2 and 0.63×10^5 K^2 for A1, 1.11×10^5 K^2 and 0.65×10^5 K^2 for A4 composites, respectively. The ratios of K_g for the higher and the lower temperature are 1.96 for A0, 1.65 for A1, and 1.71 for A4, respectively. These values are close to the theoretical ratio value 2, which corresponds to the change from regime I to regime II.[29] The value of U^* at regime I (11.22 kJ/mol for A0, 9.59 kJ/mol for A1, and 9.52 kJ/mol for A4) is lager than that at regime II (6.31 kJ/mo for A0, 6.18 kJ/mol for A1, and 5.78 kJ/mol for A4). Although U^* is usually set to be constant value (6.3 kJ/mol), Hoffman et al.[29] thought the best fits value of U^* tends to vary between 4.2–16.7 kJ/mol, they have also noted that increasing the

TABLE V
Hoffman–Lauritzen Crystallization Parameters of A0, A1, and A4 Composites

			I, III			II		
Sample	T_∞ (K)	T_m (K)	U^* (kJ/mol)	$K_g \times 10^{-5}$ (K^2)	r^2	U^* (kJ/mol)	$K_g \times 10^{-5}$ (K^2)	r^2
A0	291	498	6.31	0.51	0.98	11.22	1.00	0.98
A1	295	499	6.18	0.63	0.98	9.59	1.04	0.98
A4	303	501	5.78	0.65	0.99	9.25	1.11	0.99

value of U^* results in evaluating a larger value of K_g.[30] For our data, substituting the constant value of U^* in (11) yields a noticeably bigger value of K_g for regime II. Moreover, compared the K_g of A0 with those of A1 and A4 at the higher or the lower temperature, it is apparent the more SCF content in composites, the faster crystallization rate is.

CONCLUSION

The crystal morphology and nonisothermal crystallization kinetics of SCF/PTT composites are investigated using the polarized optical microscope (POM) and differential scanning calorimeter (DSC). According to the morphology analysis, SCF acting as nucleation agent not only accelerates the crystallization rate but also decreases the dimension of the crystals; moreover, it can bring banded spherulites due to the interaction between the SCF and PTT molecular chains at the cooling rate of 1°C/min. The modified Avrami theory, Ozawa equation and the method developed by Mo are all successful in describing the nonisothermal crystallization process of SCF/PTT composites. At the primary stage of the nonisothermal crystallization process of A0, A1, and A4, the change of the n values indicates that the nonisothermal crystallization process of the composite is more complicated than pure PTT, and the crystals in composites have more growth dimensions. The results of $t_{1/2}$ and K_c suggest SCF acting as nucleation agent can arouse and accelerate crystallization of the composites and decrease the dimension of the crystals. Moreover, the effective activation energy calculated by differential iso-conversional method suggests the composites with more SCF have higher crystallization ability than that with less SCF, which is also confirmed by the results of K_g calculated by the Hoffman–Lauritzen theory. It should be noted that SCF can bring banded spherulites due to the interaction between the SCF and PTT molecular chains.

References

1. Yang, J.; Sidoti, G.; Liu, J.; Geil, P. H.; Li, C. Y.; Cheng, S. Z. D. Polymer 2001, 42, 7181.
2. Wu, J.; Schultz, J. M.; Samon, J. M.; Pangelinan, A. B.; Chuah, H. H. Polymer 2001, 42, 7141.
3. Chuah, H. H. Macromolecules 2001, 34, 6985.
4. Grebowicz, J. S.; Brown, H.; Chuah, H.; Olvera, J. M.; Wasiak, A.; Sajkiewicz, P.; Ziabicki, A. Polymer 2001, 42, 7153.
5. Dangseeyun, N.; Supaphol, P.; Nithitanakul, M. Polym Test 2004, 23, 187.
6. Wang, B. J.; Li, C. Y.; Hanzlicek, J.; Cheng, S. Z. D.; Geil, P. H.; Grebowicz, J.; Ho, R. M. Polymer 2001, 42, 7171.
7. He, X. Q.; Yang, D. C.; Xie, D. M. Chem J Chin Univ (China) 2005, 12, 2379.
8. Apiwanthanakorn, N.; Supaphol, P.; Nithitanakul, M. Polym Test 2004, 23, 817.
9. Ho, R. M.; Ke, K. Z.; Chen, M. Macromolecules 2000, 33, 7529.
10. Chuah, H. H. Polym Eng Sci 2001, 41, 308.
11. Hong, P. D.; Chung, W. T.; Hsu, C. F. Polymer 2002, 43, 3335.
12. Dangseeyun, N.; Srimoaon, P.; Supaphol, P.; Nithitanakul, M. Thermochimica Acta 2004, 409, 63.
13. Xue, M. L.; Sheng, J.; Yu, Y. L.; Chuah, H. H. Eur Polym J 2004, 40, 811.
14. Supaphol, P.; Dangseeyun, N.; Srimoaon, P. Polym Test 2004, 23, 175.
15. Liu, Z. J.; Chen, K. Q.; Yan, D. Y. Eur Polym J 2003, 39, 2359.
16. Chen, E. J. H, Hsiao, B. S. Polym Eng Sci 1992, 32, 280.
17. Li, T. Q.; Zhang, M. Q.; Zhang, K.; Zeng, H. M. Polymer 2000, 41, 161.
18. Ye, L.; Friedrich, K.; Kästel, J.; Mai, Y. W. Comp Sci Tech 1995, 54, 349.
19. Chi, W.; Liu, C. R. Polymer 1999, 40, 289.
20. Sari, N.; Sinmazcelik, T. Mater Design 2007, 28, 351.
21. Lu, M.; Ye, L.; Mai, Y. W. Comp Sci Technol 2004, 64, 191.
22. Huang, H.; Gu, L. X.; Ozaki, Y. Polymer 2006, 64, 104.
23. Jeziorny, A. Polymer 1978, 19, 1142.
24. Liu, M. Y.; Zhao, Q. X.; Wang, Y. D.; Zhang, C. G.; Mo, Z. S.; Cao, S. K. Polymer 2003, 44, 2537.
25. Choe, C. R, Lee, K. H. Polym Eng Sci 1989, 29, 801.
26. Ozawa, T. Polymer 1971, 12, 150.
27. Yuan, Q.; Awate, S.; Misra, R. D. K. Eur Polym J 2006, 42, 1994.
28. Xu, G.; Shi, W. F.; Hu, P.; Mo, S. P. Eur Polym J 2005, 41, 1828.
29. Hoffman, J. D.; Davis, G. T.; Lauritzen, J. I., Jr. In: Treatise on Solid State Chemistry, Vol. 3, N. B.Hannay, Ed.; Plenum: NY, 1976; p 479.
30. Vyazovkin, S.; Sbirrazzuoli, N. Macromol Rapid Commun 2004, 25, 733.
31. Vyazovkin, S.; Dranca, I. Macromol Chem Phys 2006, 207, 20.